Ultrathinning-Induced Surface Phase Separation of Polystyrene/Poly(vinyl methyl ether) Blend Film

Keiji Tanaka, Jeong-Sik Yoon,† Atsushi Takahara, and Tisato Kajiyama*

Department of Chemical Science & Technology, Faculty of Engineering, Kyushu University, 6-10-1 Hakozaki, Higashi-ku, Fukuoka 812, Japan

Received August 19, 1994®

ABSTRACT: Polystyrene/poly(vinyl methyl ether) (PS/PVME) blend films were prepared on hydrophilic SiO substrates by a dip-coating method from toluene solution. The phase-separation temperature of the (PS/PVME) blend films decreased with decreasing film thickness. The (PS/PVME) two-dimensional ultrathin film with a thickness comparable to the dimension of twice the radius of gyration of an unperturbed PVME chain did not show any distinct cloud point. Secondary ion mass spectroscopic (SIMS) measurement for the perdeuterated polystyrene/PVME (dPS/PVME) thin film revealed the selective adsorption of the dPS segments on the hydrophilic substrate in order to minimize the polymer–substrate interfacial free energy. X-ray photoelectron spectroscopic (XPS) measurement showed the enrichment of PVME at the air–polymer interface due to its lower magnitude of surface free energy compared with that of PS. However, the PVME weight fraction at the air-facing surface started to decrease with decreasing film thickness for thickness less than ca. 30 nm. Atomic force microscopic (AFM) observation revealed that the (PS/PVME) two-dimensional ultrathin film with a thickness of 25 nm was in an apparent phase-separated state forming droplet-like domains 200–500 nm in diameter and 20–40 nm in height. Scanning viscoelasticity microscopic (SVM) observation revealed that the droplet-like domains were composed of a PVME-rich phase. These results clearly indicated that the spinodal point decreased below room temperature with decreasing film thickness for thickness less than ca. 30 nm. The formation of the phase-separated domains can be explained by factors such as the negative spreading coefficient of PVME on the PS matrix and the large negative conformational entropy of a PVME chain against stretching.

Introduction

The miscibility of binary polymeric mixtures has been extensively investigated for the past few decades, both experimentally and theoretically, due to its role in blend morphology and associated mechanical properties.[1–6] Also, the surface structure of polymer blend films has been investigated over the past decade by several groups due to its importance in controlling morphology, adhesion, and wetting.[7–13] In most cases, these experiments try to understand the surface of the bulk samples. However, for polymeric blend thin films, the air–polymer and the polymer–substrate interfaces remarkably influence the molecular aggregation structure and phase-separation behavior, because polymer chains at the air–polymer and the polymer–substrate interfaces are in an unsymmetrical environment in comparison with that within the film. Reich and Cohen investigated the phase-separation temperature of polystyrene/poly(vinyl methyl ether) (PS/PVME) thin films with thicknesses of a few microns to 50 nm.[14] They revealed that the thickness effect on the phase-separation temperature was noticeable when the film thickness was smaller than 1 μm and that this effect was substrate dependent. The phase-separation temperature of (PS/PVME) thin film formed on a gold substrate increased with decreasing film thickness due to the geometrical effect of the thin film, whereas a decrease of the phase-separation temperature of (PS/PVME) was observed for the thin film formed on glass. This result for (PS/PVME) thin film formed on glass was explained by the selective adsorption of PS on glass in addition to the geometrical effect. Kraush and co-workers investigated the film thickness dependence of the spinodal wave for a binary polymeric blend.[15] They revealed that the spinodal wave originating from the polymer–substrate interface was remarkable when the film thickness was smaller than 1 μm. Also, the interference of the spinodal waves originating from the two interfaces, the air–polymer and the polymer–substrate interfaces, was observed. Moreover, the offset of the spinodal waves originating from the two interfaces was confirmed when the film thickness was smaller than 500 nm. Thus, it is expected that the film thickness effect on the molecular aggregation structure of a binary polymeric blend will become noticeable when the film thickness is smaller than 1 μm.

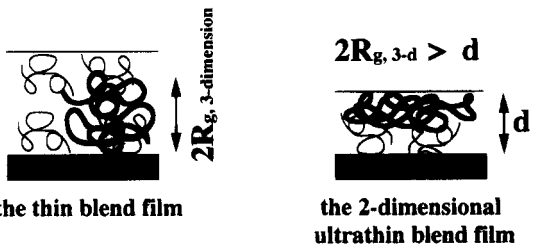

Figure 1. Schematic representation of the conformation of polymer chains in the thin film and the two-dimensional ultrathin blend film.

Polymeric films whose thicknesses are less than twice the radius of gyration of an unperturbed chain, $2R_g$, can be defined as two-dimensional ultrathin films.[16] Thus, polymeric blend films with thicknesses less than the dimension of $2R_g$ of the longest component can be defined as two-dimensional ultrathin blend films. Figure 1 shows a schematic representation of a polymer chain conformation in a thin blend film and a two-dimensional ultrathin blend film. A flexible polymer chain in an ultrathin film is in a nonequilibrium state, since the conformational entropy of an individual chain is reduced in comparison with that in a three-dimensional solid state.[17] Since, polymeric chains at the interface, in general, are thermally unstable due to more

† On leave from the Korea Institute of Footwear Technology (KIFT).

* Author to whom correspondence should be addressed.

® Abstract published in *Advance ACS Abstracts,* January 15, 1995.

0024-9297/95/2228-0934$09.00/0

Table 1. Characterizations of PS and PVME Used in This Study

	M_n	M_w/M_n	$2R_g$/nm	γ/mJ·m^{-2}	T_g/K
PS	26.6K	1.09	8.9	40.2	372
PVME	38.8K	1.98	14.6	36.0	249

vigorous thermal molecular motion and different surface free energy, the molecular aggregation structure in the two-dimensional ultrathin film of a binary polymeric blend must be greatly different from that in a thick film. However, the molecular aggregation structure in a two-dimensional ultrathin film of a binary polymeric blend has not been investigated. The purpose of this study is to reveal the surface structure of the two-dimensional ultrathin film of the polystyrene/poly(vinyl methyl ether) (PS/PVME) blend.

Experimental Section

Materials. The polymers used in this study were poly(vinyl methyl ether) (PVME) and monodisperse polystyrene (PS). PVME, which was purchased from Scientific Polymer Products, Inc., was reprecipitated from toluene into *n*-heptane and vacuum-dried. Prior to use, this procedure was repeated. PS was prepared, using standard procedures, by a living anionic polymerization at 293 K using *sec*-BuLi as initiator. Table 1 shows characterizations of PS and PVME in a three-dimensional state. The number-average molecular weight, M_n, and the molecular weight distribution, M_w/M_n, were determined via gel permeation chromatography (GPC) with polystyrene standards. The radius of gyration of an unperturbed chain was calculated by

$$R_g = (Nb^2/6)^{1/2} \quad (1)$$

where N is the degree of polymerization and b is the average statistical segment length. The magnitudes of b_{PS} and b_{PVME} were 0.68[18] and 0.69 nm,[19] respectively. The surface free energy, γ, was determined by static contact angle measurement on the basis of Owens' procedure.[20] The glass transition temperature, T_g, was measured by differential scanning calorimetry (DSC).

Film Preparation. A (PS/PVME) blend solution was prepared by mixing individual toluene solutions of PS and PVME. The (PS/PVME) blend thin films were prepared by a dip-coating method as follows. A hydrophilic silicon monoxide (SiO) coated substratum (γ = 67.7 mJ·m^{-2}) was immersed into the toluene solution of the polymers at a rate of 1 mm·s^{-1}. Then the substratum was maintained in the solution for 1 min. Finally, the substratum was drawn upward from the solution at a rate of 1 mm·s^{-1}. The film thickness was evaluated as follows. After a crater was formed in the polymer film by ion beam etching, its step height, which could be defined as the film thickness, was measured by atomic force microscopic (AFM) and/or scanning electron microscopic (SEM) observation. Also, the film thickness was evaluated with the Lambert–Beer law on the basis of the relationhip between the film thickness and the IR absorbance of 750 cm^{-1} corresponding to PS. The film thickness measured by AFM and/or SEM was in good agreement with that by IR absorbance. In the case of the ultrathin film, the relationship between the solution concentration and the film thickness was plotted, and the thickness of the ultrathin film was estimated by an extrapolation of the concentration to the corresponding one. The film thickness was controlled by the concentration of the solution.[14] The blend ratio in the film was designated as (PS/PVME) (weight/weight), where (weight/weight) was the ratio in solution.

Cloud Point Determination. The bulk (PS/PVME) film prepared from the toluene solution was transparent because of the phase mixing state at room temperature. The cloud point[21] of the (PS/PVME) thin film was determined from the temperature dependence of the light transmittance through the blend thin film at a heating rate of 1.5 K·min^{-1}.

Characterization of the Polymer–Substrate Interface. Depth profiling of the blend thin film was carried out with a secondary ion mass spectroscopic (SIMS)[22] measurement. The blend solution was prepared by blending a PVME solution with a perdeuterated polystyrene (dPS) solution, and then the (dPS/PVME) thin film was prepared by the above-mentioned procedure for SIMS measurement. A platinum layer with a thickness of 10 nm was sputter-coated on the surface of the (dPS/PVME) thin film in order to avoid a charging of the specimen during SIMS measurement. The SIMS analysis was performed using a SIMS 4000 (Seiko Instruments Inc.-Atomika Analysetechnik GmbH). The incident beam of oxygen ions, at 3.0 keV and with a current measured at the ion beam of 35 nA, was focused onto a 200 μm × 200 μm area of the specimen surface.

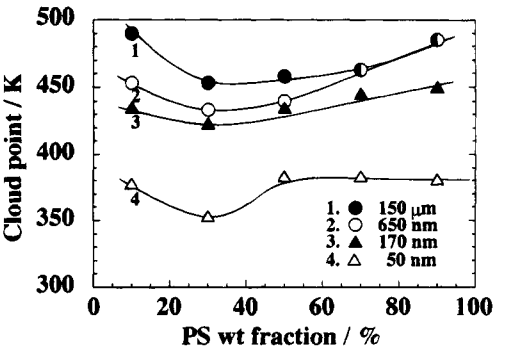

Figure 2. PS weight fraction dependence of the cloud point for the (PS/PVME) thin film as a function of the film thickness. The (PS/PVME) two-dimensional ultrathin film with the thickness of 25 nm did not show any distinct cloud point.

Surface Characterization. The surface chemical composition of the (PS/PVME) thin film was evaluated on the basis of X-ray photoelectron spectroscopic (XPS)[10] measurement. The XPS spectra were obtained with an ESCA 750 (Shimadzu Co. Ltd.) at room temperature. The XPS measurement was performed under conventional conditions with a Mg Kα source. The emission angle of photoelectrons was 90°. Thus the analytical depth of XPS for the (PS/PVME) blend film was ca. 10.5 nm using the magnitude of the inelastic mean free path of photoelectrons in solids evaluated from Ashley's equation.[23]

The surface morphology of the (PS/PVME) thin film was investigated on the basis of AFM[24] observation. The AFM images were obtained with an SFA 300 with an SPI 3700 controller (Seiko Instruments Industry Co. Ltd.) at room temperature. The AFM cantilever used was microfabricated from Si_3N_4 and its spring constant was 0.022 N·m^{-1}. AFM imaging was carried out at a repulsive force of 0.021 nN.

In order to evaluate the surface mechanical properties of the (PS/PVME) blend film, two-dimensional mapping of the dynamic modulus on the blend film surface was performed with a scanning viscoelasticity microscope (SVM) which was designed by the authors.[25]

Results and Discussion

Film Thickness Effect on the Cloud Point. Figure 2 shows the PS weight fraction dependence of the cloud point for the (PS/PVME) thin film as a function of the film thickness. The cloud point of the (PS/PVME) thin film decreased with decreasing film thickness. Reich and Cohen explained that a decrease of the cloud point for (PS/PVME) thin films with thicknesses of 1 μm to 50 nm resulted from the selective adsorption of the PS segments on the hydrophilic substrate.[14] The discrepancy of the cloud point from those of the thick films became more pronounced for the (PS/PVME) thin films with the thickness of 50 nm. The (PS/PVME) two-dimensional ultrathin films with the thickness of 25 nm did not show any distinct cloud point. The film thickness of 25 nm is comparable to the magnitude of $2R_g$ of a PVME chain, which is smaller than that in a three-dimensional blend film. On the other hand, in the case of the film with the thickness of 50 nm, $2R_g$ of a PVME chain in the thin film is almost equal to that in a three-

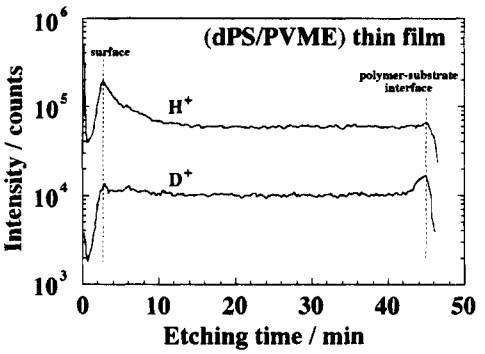

Figure 3. SIMS depth profile of H^+ and D^+ ions for the (dPS/PVME) (50/50 w/w) thin film with 340 nm thickness.

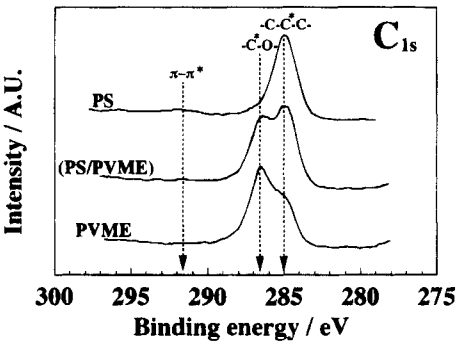

Figure 4. XPS C_{1s} core-level spectra of the (PS/PVME) (50/50 w/w) blend and PS and PMMA homopolymers at the emission angle of the photoelectrons of 90°. All neutral C_{1s} peaks were assigned a binding energy of 285.0 eV to correct for the charging energy shift. The spectral intensities are normalized using the intensity for the (PS/PVME) blend.

dimensional blend film. Also, phase contrast microscopic (PCM) observations revealed that the PS domain size in the (PS/PVME) blend films which were annealed above the cloud point decreased with decreasing film thickness.

Depth Profiling. SIMS depth profiling of the blend thin film was carried out to characterize the polymer–substrate interface. Figure 3 shows the SIMS depth profile of the as-cast 340 nm thick (dPS/PVME) thin film. A platinum layer with a thickness of 10 nm was etched for ca. 2.5 min. The dashed vertical lines at lower and higher etching times correspond to the air–polymer and the polymer–substrate interfaces, respectively. Figure 3 apparently shows the increase in concentration of protons at the air–polymer interface. On the other hand, the increase in concentration of deuterium ions was observed at the polymer–substrate interface. Since polystyrene was deuterated, protons were present only in PVME. Thus, the SIMS depth profile shows an enrichment of PVME segments with a smaller surface energy compared with that of dPS at the air–polymer interface. On the other hand, the selective adsorption of the dPS segments on the hydrophilic substrate was observed. These results can be explained by the minimization of the air–polymer and the polymer–substrate interfacial free energy. Since polystyrene and perdeuterated polystyrene have similar physicochemical properties, the PS segments would be concentrated at the hydrophilic substrate for the (PS/PVME) thin film.

Film Thickness Effect on Surface Composition. To investigate the effect of the film thickness on the surface composition of the (PS/PVME) (50/50 w/w) blend film, XPS measurements were performed. Figure 4 shows the XPS C_{1s} spectra of the as-cast thin film for

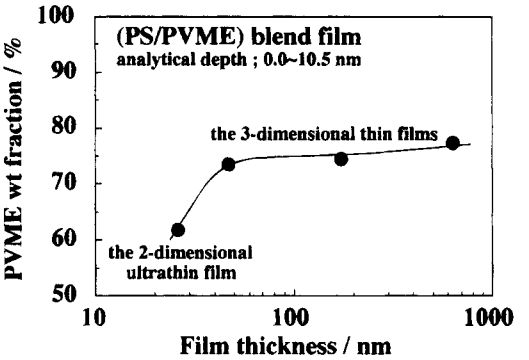

Figure 5. Film thickness dependence of the average PVME weight fraction at AFS for the (PS/PVME) blend film prepared from (PS/PVME) (50/50 w/w) toluene solution.

the (PS/PVME) blend and the PS and PVME homopolymers at the emission angle of photoelectrons of 90°. The C_{1s} peak corresponding to the neutral carbon was observed at 285.0 eV. The C_{1s} peak observed at 286.5 eV was assigned to the ether carbon. Also, the C_{1s} shake-up peak corresponding to the $\pi-\pi^*$ transition of the benzene ring was observed at 291.5–292.0 eV. The surface composition, the average PVME weight fraction, was evaluated on the basis of the ratio of the XPS peak intensities for the neutral and the ether carbons. The C_{1s} spectra for the (PS/PVME) blend film were deconvoluted into the three peaks corresponding to the neutral carbon, the ether carbon, and the shake-up of $\pi-\pi^*$ of the benzene ring by a standard nonlinear curve fitting. Then the PVME weight fraction, ω, was calculated by

$$\frac{I_{C-O}}{I_{total}} = \frac{2\omega/M_{VME}}{8(1-\omega)/M_S + 3\omega/M_{VME}} \quad (2)$$

where I_i is the integrated intensity of each core-electron photoemission spectrum. M_S and M_{VME} are the molecular weights of the styrene and vinyl methyl ether repeat units, respectively. Figure 5 shows the film thickness dependence of the average PVME weight fraction at the air-facing surface (AFS) for the (PS/PVME) (50/50 w/w) blend films. Figure 5 apparently shows the enrichment of the PVME segments at AFS. This result agreed with the SIMS result. The degree of the surface enrichment of PVME for the 25 nm thick (PS/PVME) two-dimensional ultrathin film was less than those of the blend thin films with thicknesses larger than 50 nm. In the case of the 25 nm thick ultrathin film prepared from a toluene solution with the blend ratio of (PS/PVME) (50/50 w/w), however, it was revealed on the basis of transmission IR measurements that the bulk composition was (PS/PVME) (62/38 w/w) due to the selective adsorption of PS. On the other hand, in the case of the three-dimensional blend films with thicknesses greater than 50 nm, the blend ratio in the film corresponded to that of the solution. It was confirmed that, although the (PS/PVME) ultrathin film had the bulk composition of (PS/PVME) (62/38 w/w), the discrepancy of the surface enrichment of PVME between the thin and ultrathin films could not be ascribed to the discrepancy of the net average composition. Thus, these results indicate that the surface molecular aggregation state of the (PS/PVME) two-dimensional ultrathin films is different from that of three-dimensional blend films.

Surface Morphology. Figures 6 and 7 show the AFM images of the as-cast 25 nm thick (PS/PVME) (62/38 w/w) ultrathin film and the as-cast 50 nm thick (PS/PVME) (50/50 w/w) thin film on the hydrophilic sub-

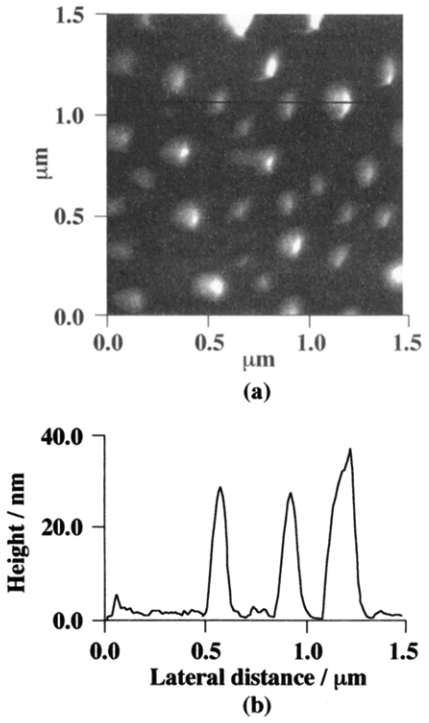

Figure 6. (a) AFM image and (b) sectional view along the line in the AFM image for the 25 nm thick (PS/PVME) (62/38 w/w) two-dimensional ultrathin film on the hydrophilic substrate. The (PS/PVME) composition in the ultrathin film was corrected on the basis of transmittance IR measurements.

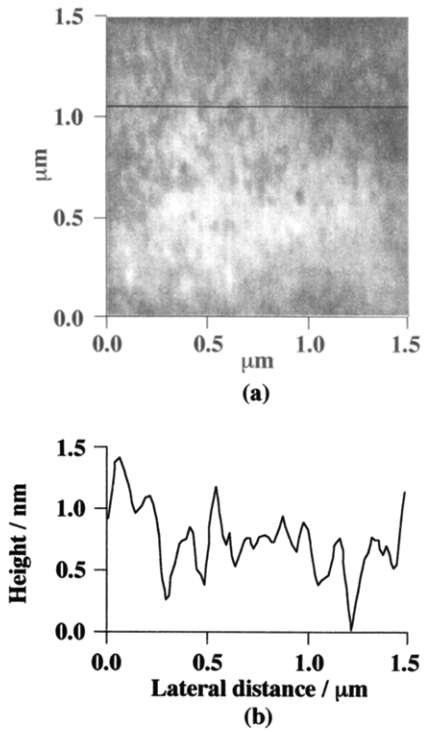

Figure 7. (a) AFM image and (b) sectional view along the line in the AFM image for the 50 nm thick (PS/PVME) (50/50 w/w) thin film on the hydrophilic substrate.

strate, respectively. The (PS/PVME) blend ratio in the ultrathin film was corrected on the basis of transmission IR measurements. AFM observations were carried out at room temperature. To confirm if the surface structure shown in Figure 6 was attributed to dewetting of the polymer, XPS measurements were performed. Since the magnitude of the ratio of the XPS peak intensities for Si_{2p} and C_{1s} was very small compared with that assuming a dewetting structure in which the matrix was

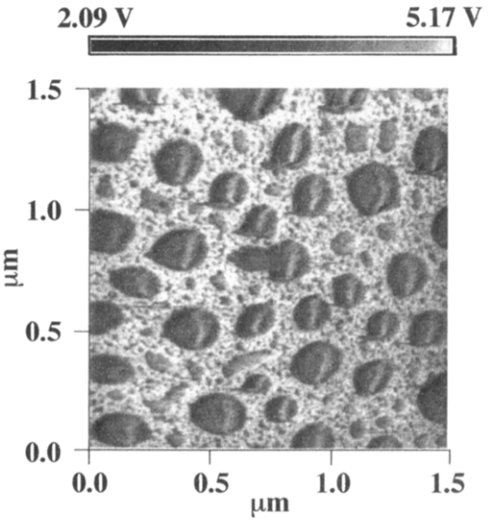

Figure 8. SVM image corresponding to the real part of the modulus for the 25 nm thick (PS/PVME) (62/38 w/w) two-dimensional ultrathin film on the hydrophilic substrate. The (PS/PVME) composition in the ultrathin film was corrected on the basis of transmittance IR measurements.

composed of the bare substrate, it was apparent that photoelectrons emitted from Si atoms decreased with polymer coverage on the substrate; that is, the substrate was covered with polymer chains. Figure 6 revealed that the (PS/PVME) two-dimensional ultrathin film was in an apparent phase-separated state in which droplet-like domains 200−500 nm in diameter and 20−40 nm in height were formed. Since the cloud point of the 50 nm thick blend film at this composition is ca. 380 K, the phase separation in the as-cast ultrathin film cannot be attributed to compositional change. Also, in the case of the ultrathin films prepared from toluene solutions with blend ratios of (PS/PVME) (30/70 w/w) and (70/30 w/w), the surface structure with the droplet-like domains was also observed. On the other hand, the AFM images of the as-cast (PS/PVME) thin films with thicknesses larger than 50 nm were flat on the scale of a few nanometers. Thus it seems reasonable to conclude that in the case of the 25 nm thick (PS/PVME) two-dimensional ultrathin film, phase separation proceeds during the solvent evaporation process even if below the bulk spinodal temperature. The characterization of the droplet-like domains was carried out using AFM observation of (PS/PVME) two-dimensional ultrathin films with different (PS/PVME) blend ratios. The apparent surface area for the droplet-like domains on the AFM image decreased with decreasing PVME weight fraction. Thus it is apparent from the AFM observation that the droplet-like domains are composed of a PVME-rich phase.

Surface Viscoelasticity. SVM observations were performed to evaluate the surface viscoelasticity of the as-cast 25 nm thick (PS/PVME) (62/38 w/w) two-dimensional ultrathin film on the hydrophilic SiO substrate. Since the bulk glass transition temperature of PS is far above room temperature whereas that of PVME is below room temperature, it is expected that the glassy PS and the rubbery PVME phases can be distinguished apparently even at the surface on the basis of the SVM observation. Figure 8 shows the two-dimensional image of the real part of the modulus for the (PS/PVME) ultrathin film at 293 K under a modulation frequency of 5 kHz and a dynamic z-axis modulation of 1.2 nm. The dark and bright regions correspond to the lower and higher real parts of the modulus, respectively. The droplet-like domains in Figure 8

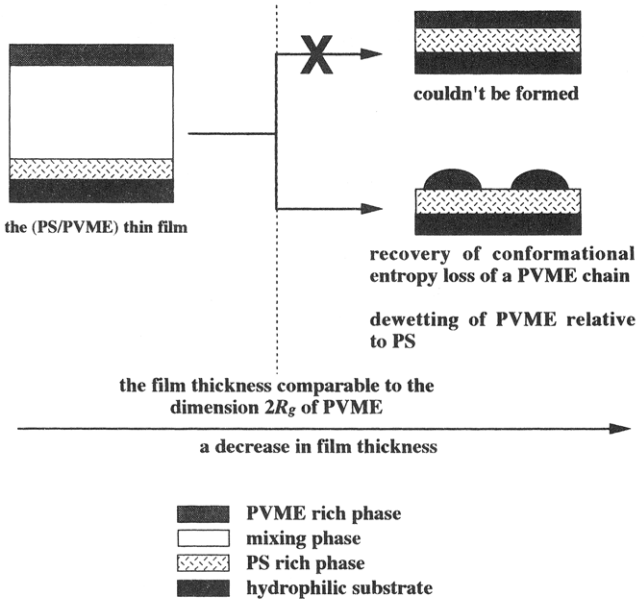

Figure 9. Schematic representation of the formation of the phase-separated surface structure for the (PS/PVME) two-dimensional ultrathin film.

completely correspond to those for the AFM image in Figure 6. Since the droplet-like domains were observed as the darker region in comparison with the brighter matrix, it is reasonable to conclude that the droplet-like domains are composed of the rubbery PVME-rich phase and also that the matrix is composed of the glassy PS phase.

Mechanism of Surface Phase Separation. When the thickness of the (PS/PVME) thin film is smaller than the magnitude of $2R_g$ of a PVME chain in a three-dimensional blend film, a PVME chain must be constrained in an extremely narrow space and then lose its conformational entropy during a nonequilibrium film formation process, even in a rubbery state at room temperature. Thus, a PVME chain tends to recover its random coil conformation. Figure 9 schematically summarizes the formation process of the phase-separated structure of the (PS/PVME) two-dimensional ultrathin film. Since the PS segments are preferentially adsorbed and expanded as a thin film onto the hydrophilic SiO substrate, the wetting property of PVME relative to PS has an important role for the formation of the (PS/PVME) two-dimensional ultrathin film. The effective spreading coefficient, S', can be expressed as follows:

$$S' = \frac{dF}{dA} \tag{3}$$

where F and A are the free energy and the area of a thin film, respectively.[26] F for a thin film with the film thickness of d, chains per unit area of n, and constant volume of $V_0 = Ad$ can be expressed as[26]

$$F = A\left\{(\gamma + \gamma_{sl} - \gamma_{so}^{d}) + \left(\frac{a}{12\pi d^2}\right) + \frac{\pi^2}{6}k_B T n\left[\left(\frac{R_0}{d}\right)^2 - 1\right]\right\} \tag{4}$$

where γ is surface free energy, a is the Hamaker constant, k_B is the Boltzmann constant, T is the absolute temperature, and R_0 is the end-to-end distance of an unperturbed chain. The first term is the negative of the macroscopic spreading parameter. The second term is the van der Waals term. Also, the last term is the free energy cost of stretching n polymer chains per unit area. In the case of $S' < 0$, the surface is only partially wet. For the (PS/PVME) two-dimensional ultrathin film with the thickness of 25 nm, S' is negative after formation of the PS thin film and then the PVME component dewets on the PS matrix. From the results obtained above, it may be concluded that the formation of the phase-separated structure in the (PS/PVME) two-dimensional ultrathin film can be explained by the following two factors: an increase of conformational entropy of the PVME segments constrained in a narrow space and the dewetting of PVME relative to PS.

Conclusion

(PS/PVME) two-dimensional ultrathin films prepared on hydrophilic substrates were in a phase-separated state even at room temperature. The phase-separated (PS/PVME) two-dimensional ultrathin films had surface structures whose PVME domains overlaid the PS thin film. The formation of the phase-separated structure can be explained by two factors: recovery of conformational entropy loss of a PVME chain and dewetting of PVME relative to PS.

References and Notes

(1) de Gennes, P.-G. *Scaling Concepts in Polymer Physics*; Cornell University Press: London, 1979.
(2) Nishi, T.; Wang, T. T.; Kwei, T. K. *Macromolecules* **1975**, *8*, 227.
(3) Nose, T. *Polym. J.* **1976**, *8*, 96.
(4) Davis, D. D.; Kwei, T. *J. Polym. Sci., Polym. Phys. Ed.* **1980**, *18*, 2337.
(5) Bates, F. S.; Wiltzius, P. *J. Chem. Phys.* **1990**, *91*, 3258.
(6) Beaucage, G.; Stein, R. S.; Koningsveld, R. *Macromolecules* **1993**, *26*, 1603.
(7) Lee, W.-K.; Ha, C.-S.; Cho, W.-J.; Takahara, A.; Kajiyama, T. *Polymer*, in press.
(8) Takahara, A.; Korehisa, K.; Takahashi, K.; Kajiyama, T. *Kobunshi Ronbunshu* **1992**, *49*, 275.
(9) Pan, D. H.-K.; Prest, W. M., Jr. *J. Appl. Phys.* **1985**, *58*, 2861.
(10) Bhatia, Q. S.; Pan, D. H.-K.; Koberstein, J. T. *Macromolecules* **1988**, *21*, 2166.
(11) Bruder, F.; Brenn, R. *Phys. Rev. Lett.* **1992**, *69*, 624.
(12) Cowie, J. M. G.; Devlin, B. G.; Mcwen, I. J. *Polymer* **1993**, *34*, 501.
(13) Hong, P. P.; Boerio, F. J.; Smith, S. D. *Macromolecules* **1994**, *27*, 596.
(14) Reich, S.; Cohen, Y. *J. Polym. Sci., Polym. Phys. Ed.* **1981**, *19*, 1255.
(15) Krausch, G.; Dai, C.-A.; Kramer, E. J.; Marko, J. F.; Bates, F. S. *Macromolecules* **1993**, *26*, 5566.
(16) Shuto, K.; Oishi, Y.; Kajiyama, T.; Han, C. C. *Polym. J.* **1993**, *25*, 291.
(17) Shuto, K.; Oishi, Y.; Kajiyama, T. *Polymer*, in press.
(18) Ballard, D. G. H.; Wignall, G. D.; Schelten, J. *Eur. Polym. J.* **1973**, *9*, 965.
(19) Beaucage, G.; Stein, R. S. *Macromolecules* **1993**, *26*, 1617.
(20) Owens, D. K.; Wendt, R. C. *J. Appl. Polym. Sci.* **1969**, *13*, 741.
(21) Nishi, T.; Kwei, T. K. *Polymer* **1975**, *16*, 285.
(22) Chujo, R.; Nishi, T.; Sumi, Y.; Adachi, Y.; Naito, H.; Frentzel, H. *J. Polym. Sci., Polym. Lett. Ed.* **1983**, *21*, 487.
(23) Ashley, J. C. *IEEE Trans. Nucl. Sci.* **1980**, *NS-27*, 1454.
(24) Albrecht, T. R.; Dovek, M. M.; Lang, C. A.; Grutter, P.; Quate, C. F.; Kuar, S. W. J.; Frank, C. W.; Pease, R. F. W. *J. Appl. Phys.* **1988**, *64*, 1178.
(25) Kajiyama, T.; Tanaka, K.; Ohki, I.; Ge, S. R.; Yoon, J. S.; Takahara, A. *Macromolecules* **1994**, *27*, 7932.
(26) Zhao, W.; Rafailovich, H.; Sokolov, J.; Fetters, L. J.; Plano, R.; Sanyal, M. K.; Sinha, K. *Phys. Rev. Lett.* **1993**, *70*, 1453.

MA9411888